Changes in the hydrogen-bonding strength of internal water molecules and cysteine residues in the conductive state of channelrhodopsin-1

Víctor A. Lórenz-Fonfría,[1,a)] Vera Muders,[2,a)] Ramona Schlesinger,[2] and Joachim Heberle[1,b)]
[1]*Experimental Molecular Biophysics, Freie Universität Berlin, 14195 Berlin, Germany*
[2]*Genetic Biophysics, Freie Universität Berlin, 14195 Berlin, Germany*

(Received 18 July 2014; accepted 4 September 2014; published online 23 September 2014)

Water plays an essential role in the structure and function of proteins, particularly in the less understood class of membrane proteins. As the first of its kind, channelrhodopsin is a light-gated cation channel and paved the way for the new and vibrant field of optogenetics, where nerve cells are activated by light. Still, the molecular mechanism of channelrhodopsin is not understood. Here, we applied time-resolved FT-IR difference spectroscopy to channelrhodopsin-1 from *Chlamydomonas augustae*. It is shown that the (conductive) P_2^{380} intermediate decays with $\tau \approx 40$ ms and 200 ms after pulsed excitation. The vibrational changes between the closed and the conductive states were analyzed in the X-H stretching region (X = O, S, N), comprising vibrational changes of water molecules, sulfhydryl groups of cysteine side chains and changes of the amide A of the protein backbone. The O-H stretching vibrations of "dangling" water molecules were detected in two different states of the protein using $H_2{}^{18}O$ exchange. Uncoupling experiments with a 1:1 mixture of H_2O:D_2O provided the natural uncoupled frequencies of the four O-H (and O-D) stretches of these water molecules, each with a very weakly hydrogen-bonded O-H group (3639 and 3628 cm^{-1}) and with the other O-H group medium (3440 cm^{-1}) to moderately strongly (3300 cm^{-1}) hydrogen-bonded. Changes in amide A and thiol vibrations report on global and local changes, respectively, associated with the formation of the conductive state. Future studies will aim at assigning the respective cysteine group(s) and at localizing the "dangling" water molecules within the protein, providing a better understanding of their functional relevance in *Ca*ChR1. © *2014 AIP Publishing LLC*. [http://dx.doi.org/10.1063/1.4895796]

I. INTRODUCTION

The complex hydrogen-bonded network of liquid water accounts for many of its unusual physico-chemical properties,[1–3] the other important factor being quantum nuclear effects of the hydrogen atoms.[3,4] Each water molecule can be involved in a maximum of four hydrogen bonds (H-bonds), two as a donor (O-H groups) and two as an acceptor (at the free electron pairs of the oxygen atom). In liquid water, the average number of H-bonds per water molecule is still controversial,[5] but generally believed to be around 3.6.[2,4] Therefore, around 10% of the time water molecules are expected to be "dangling" waters, i.e., with one or two O-H groups free from H-bonding.[3]

The distribution and dynamics of H-bonds in water can be probed by vibrational spectroscopy, affecting the vibration frequency, line-shape, and intensity of the stretching of the O-H group. The frequency of the O-H stretching vibration has been shown empirically to inversely correlate with the O···O distance and the H-bond strength.[6,7] The more red-shifted an O-H stretching mode appears, the stronger this group is H-bonded to nearby molecules, an expectation confirmed by simulations.[8,9] In addition, the full-width at half-maximum (FWHM) of the resulting band increases with the strength of the H-bond.[10,11] The broadening is mostly ascribed to increased anharmonic couplings to low-frequency modes and more effective vibrational relaxation. The integrated absorption coefficient of the O-H stretching also increases with the strength of the H-bond. This increase is explained by strengthened polarization of the O-H bond.[11,12] To lesser extend, the O-H frequency is affected as well by intramolecular (and intermolecular) vibrational coupling between the O-H transition dipole moment of the same (and surrounding) molecule(s).[3] This coupling results in the well-known asymmetric and symmetric modes at 3756 and 3657 cm^{-1} of H_2O in the gas phase. Both the intramolecular and intermolecular coupling can be effectively turned off by isotopic dilution experiments, using a H_2O/D_2O mixture.[3,12]

In liquid water, the O-H stretching is characterized by a very broad absorption band in the infrared region, extending from 3700 to 2800 cm^{-1},[13] illustrating the heterogeneous nature of H-bonds in water.[8] The O-H (O-D) stretch of HOD diluted in D_2O (H_2O), a model system to uncoupled O-H (O-D) vibrations, peaks at ~3400 cm^{-1} (~2500 cm^{-1}).[3,12] The frequency of the O-H stretch of a water molecule fluctuates in time, a process known as spectral diffusion that can be used to probe molecular dynamics. Ultrafast vibrational experiments probing the O-H stretching lead to the conclusion that "dangling" O-H groups are transient species in water. They spectrally diffuse in 200 fs to an H-bonded form and can

[a)] Víctor A. Lórenz-Fonfría and Vera Muders contributed equally to this work.
[b)] Author to whom correspondence should be addressed. Electronic mail: joachim.heberle@fu-berlin.de

be considered as intrinsically unstable forms.[14] Their lifetime is faster than the vibrational relaxation of the O-H group,[15] which, therefore, only very occasionally senses a pure H-bond free from its environment. Indeed, diluted HOD in phenol gives a narrow band at ∼3600 cm^{-1} with a 15-20 cm^{-1} width (FWHM),[12] while those from formal dangling O-H groups in water give a considerable broader band of ∼100 cm^{-1} width, according to spectral simulations.[3]

Dangling O-H groups of water are expected to be more numerous and stable at hydrophobic interfaces, such as the water-air interface, due to geometric constrains.[16] In fact, vibrational sum-frequency spectroscopy, a surface-sensitive technique, has shown that the interface is particularly enriched in dangling O-H groups with a characteristic vibration at ∼3680 cm^{-1}.[17,18] This band is relatively narrow (∼30 cm^{-1})[17,18] with a line width partially limited by the fast reformation of H-bonds at the interface due to fast reorientation of interface water molecules.[18] Dangling O-D groups at the water-air interface oscillate at ∼2740 cm^{-1} and exhibit narrow bandwidths (11–14 cm^{-1}).[19]

Protonated water clusters (comprising 2-27 water molecules) have also been intensively studied by vibrational spectroscopy.[20,21] They contain a large number of dangling O-H groups at the outer shell of the cluster, characterized by O-H frequencies at 3695 and 3715 cm^{-1}, and bands of narrow width (∼15 cm^{-1}). The lower and the higher wavenumber bands have been assigned to dangling O-H groups accepting either two or only one H-bond at the oxygen atom.[20] As a comparison, the uncoupled O-H (O-D) stretch of water in the gas phase, the simpler model for non H-bonded water, appears at 3707 cm^{-1} (2724 cm^{-1}).[3]

Water molecules fill cavities in proteins and are located in putative proton transfer pathways.[22] Geometric constrains can lead to unsatisfied H-bonds and, therefore, to dangling and weakly H-bonded O-H groups in proteins. Their detection by vibrational spectroscopy is compromised by the large background absorption from the bulk water hydrating the protein and the high number of active vibrational modes of proteins. Difference spectroscopy solves both technical issues, revealing selectively "functionally active" vibrations, i.e., those changing between two states of a protein. Because of the natural occurrence of O-H groups in proteins, in the side chains of threonine, serine, and tyrosine, the assignment of O-H vibrations to internal waters relies on the ∼11 cm^{-1} spectral downshift when using $H_2{}^{18}O$ as a solvent, as shown by pioneering studies on bacteriorhodopsin (BR).[23–25] Briefly, dangling and weakly H-bonded waters in proteins show bands between 3700 and 3600 cm^{-1} with a bandwidth of 6-20 cm^{-1}. This experimental approach was later extended to experiments in $D_2{}^{16}O$ and $D_2{}^{18}O$, in the less congested X-D stretching region, which benefits from slightly larger isotopic downshifts (∼14 cm^{-1}) and narrower bands.[26] This opens the way to the simultaneous detection of very weakly to very strongly H-bonded active waters in a variety of different proteins.[27–29] Numerous cryogenic studies on O-H stretching changes of internal waters in retinal proteins followed[28,30] and were successfully extended to other photosensitive proteins.[31] Later, dangling and weakly H-bonded water molecules have been also detected at room temperature.[32–34] Changes in the D-O-D bending of water molecules have been detected, as well.[35] It was shown that the exchange of the protein solvent from $H_2{}^{16}O$ to $H_2{}^{18}O$ is enough to detect dangling waters in the dark state of BR, without the need to induce a photoreaction.[36]

In the present work, another class of the large family of retinylidene proteins was studied. Channelrhodopsins (ChRs) are light-gated ion channels, the first and so far the only ones known in nature.[37] Light-driven passive conductance for cations by ChRs was proven in ground-breaking electrophysiological experiments on *Xenopus* oocytes and HEK cells expressing ChR1 and ChR2 from the algae *Chlamydomonas reinhardtii*.[38] ChRs belong to the family of microbial rhodopsins, characterized by containing seven transmembrane helices and harboring as a chromophore a retinal molecule covalently bound to a lysine side chain to form a protonated Schiff base (SB).[39] The light-gated ion conductivity of ChRs forms part of the phototaxis machinery of green unicellular algae, involved in attractive and repellent responses to the wavelength, intensity, and direction of the surrounding light.[40] When ChRs are heterologously expressed in neuronal cells, light can be used to depolarize the cell membrane and, thus, ChRs can be used to elicit action potentials.[41]

Channelrhodopsin-2 from *C. reinhardtii*, *Cr*ChR2, is the best characterized ChR so far, both by electrophysiological and spectroscopic studies, as recently reviewed.[42,43] *Cr*ChR2 absorbs maximally at ∼470 nm and shows a photocycle comprising a minimum of four intermediate states: $P_1{}^{500}$, $P_2{}^{390}$, $P_3{}^{520}$, and $P_4{}^{480}$, where the superscript indicates the approximate absorption maximum of the retinal in nm. $P_1{}^{500}$ is an early red-shifted intermediate, akin to the K intermediate observed in all microbial rhodopsins. $P_2{}^{390}$ represents an intermediate with deprotonated SB, i.e., an M-like intermediate. $P_3{}^{520}$ is formed after reprotonation of the SB. Finally, $P_4{}^{480}$ represents an intermediate with a chromophore conformation and environment similar to the dark state. Correlation of photocurrents measured by electrophysiology and optical data suggests that the late $P_2{}^{390}$ and $P_3{}^{520}$ intermediates are conductive states, while $P_1{}^{500}$ and the early $P_2{}^{390}$ intermediates are nonconductive states and $P_4{}^{480}$ intermediate represents a desensitized state.[43]

The only ChR whose 3D structure has been resolved to atomic resolution is a chimera construct from *Cr*ChR1 and *Cr*ChR2 (C1C2).[44] Recently, the first report on active internal water molecules on a ChR was published, performed on the C1C2 chimera.[45] Light-induced FT-IR spectroscopy revealed changes in water O-D vibrations upon illumination at 77 K, i.e., between the closed dark and the early $P_1{}^{500}$ state. An unusually large number of active water molecules were identified as compared to other microbial rhodopsins.[27,46] One of them was assigned by mutagenesis to form part of the H-bonding network that stabilizes the protonated SB.

A recent homology cloning survey identified several new ChRs in *Chlamydomonas*.[47] Among them, ChR1 from *Chlamydomonas augustae*, *Ca*ChR1, shows some favorable properties to compete with *Cr*ChR2 as a tool to depolarize the membrane potential of a host cell by light: a red-shifted absorption maximum (see Fig. S1 of the supplementary material[59]) and a lower inactivation level under sustained illumination.[47] This lower inactivation allows achieving

light-driven membrane depolarization even at lower expression levels in the cell. The possibility to use a more red-shifted excitation light, minimizes light scattering of biological tissues and allows for deeper penetration depth into the tissue of targeted cells. Another favorable property of *Ca*ChR1 is that, in contrast to *Cr*ChR2, the P_2^{380} intermediate is accumulated under continuous illumination,[48] facilitating its biophysical characterization. The lifetime of the P_2^{380} state of *Ca*ChR1 correlates with the time domain for passive channel current measured in HEK cells.[49] Consequently, the P_2^{380} intermediate represents the conductive state of *Ca*ChR1, in contrast to *Cr*ChR2 where the P_3^{520} intermediate is the main conductive state. Here, we show that the conductive P_2^{380} state of *Ca*ChR1 exhibits large conformational changes in the protein backbone, as inferred from the analysis of amide A, I, and II vibrations, as well as H-bonding changes in the sulfhydryl group (S-H) of cysteine side chains. Moreover, we provide a detailed analysis on the O-H (and O-D) stretching vibrations of weakly H-bonded internal water molecules. Namely, by isotopic uncoupling experiments, we characterized the natural vibration frequency of the two O-H stretches of a water molecule in the dark and in the P_2^{380} state. This is the first time that water molecules are detected and characterized in the conductive state of a ChR. An additional novelty is the use of isotopic uncoupling experiments to quantitatively infer the frequency of strongly H-bonded O-H groups of water in proteins.

II. MATERIALS AND METHODS

A. Steady-state FT-IR spectroscopy

*Ca*ChR1 was cloned, expressed and purified as described.[48] *Ca*ChR1 was concentrated to 5-10 mg/ml in 5 mM NaCl, 5 mM Hepes, pH 7.4 and 0.05% DDM. 2-5 μl was dried on top of a BaF_2 window. The protein film was rehydrated from the vapor phase from 3 μl of a glycerol/water solution (2/8 w/w corresponding to a relative humidity of ~98%) placed near the film.[50] The hydrated film was sealed with a second window using a 1 mm thick spacer. We used either normal water (99.7% ^{16}O atoms), heavy water (99.8% D atoms), or ^{18}O labeled water (97% ^{18}O atoms). When mixed with D_2O, we used perdeuterated glycerol (98% D atoms). For O-H uncoupling experiments we used a 1:1 mixture of H_2O and D_2O (v/v). Protein hydration was sufficient as seen by the absorbance of the IR spectrum of the hydrated film (see Fig. S2 of the supplementary material[59]). We could also confirm that contamination with O-H was negligible (<5% H atoms) in D_2O experiments, as judged by the relative absorbance of O-H and O-D stretching bands (see Fig. S2 of the supplementary material[59]). Light-induced IR difference spectra were measured in transmission mode, using a commercial FT-IR spectrometer (Vertex 80v, Bruker) running at a spectral resolution of 2 cm^{-1}. The samples were kept in the dark for 10 s, and subsequently illuminated for 10 s by an LED emitting blue-green light (λ_{max} = 505 nm). Data acquisition was performed in the last 5 s in dark and light. The process was automatically repeated to a final of 3000 co-added scans. The sample holder was kept at 25 °C by a circulating water bath (F25, Julabo).

Temperature-induced IR difference spectra of H_2O, D_2O and $H_2{}^{18}O$ were measured in attenuated total reflection (ATR) mode, using a single reflection diamond cell (Resultec, Germany). A water-circulating holder connected to a thermostated bath was used to change the temperature from 25 °C to 27 °C. The penetration depths of the evanescent wave in ATR spectroscopy is wavenumber-dependent, which needs to be accounted for the quantitative comparison to transmission experiments. We calculated the wavenumber dependence of the effective penetration using Harrick's equations for the thick-weak absorber approximation,[51] using the published refractive indices spectra of H_2O and D_2O (http://www.ualberta.ca/~jbertie/JBDownload.HTM)[13,52] as shown in Fig. S3 of the supplementary material.[59] For $H_2{}^{18}O$, we used the refractive index spectrum of H_2O, with wavenumbers rescaled by 0.997 due to the change in reduced mass. The experimental absorption difference ATR-IR spectra from the heating of water was divided by the calculated effective penetration to cancel wavenumber-dependent penetration effects.

B. Spectral post-processing

To improve the signal-to-noise ratio when analyzing the X-H (X = O, N, S) spectral region, FT-IR difference spectra above 1800 cm^{-1} were post-processed to 4 cm^{-1} resolution in the Fourier domain, using a Triangle filter of suitable cut-off, in a home-made routine running in Matlab. For the detailed analysis of the O-H and O-D stretching regions, the FT-IR difference spectra were corrected for heat-induced spectral changes by subtracting the temperature-induced FT-IR difference spectrum of liquid water with an appropriate scaling factor. Further improvement of the baseline was accomplished by applying a Fourier filter in a home-made routine running in Matlab. We used a Gaussian of 80 cm^{-1} for baseline correction of the S-H region of 40 cm^{-1} width for the O-H stretch region and of 20 cm^{-1} width for the O-D stretch region.

C. Time-resolved rapid-scan FT-IR spectroscopy

A hydrated film of *Ca*ChR1 was excited every 100 s with a 10 ns blue (490 nm) laser pulse from an OPO (optical parametric oscillator) driven by the third harmonic of a Nd:YAG laser. After photo-excitation, double-sided interferograms were recorded for 94 s in the forward and backward direction. The process was repeated 500 times (~14 h of data collection) for signal-to-noise improvement. Interferograms were scanned at an optical retardation corresponding to a spectral resolution of 8 cm^{-1}, and at a mirror speed requiring 13 ms to complete a double-side interferogram (modulation of the internal HeNe laser of 200 kHz). Data points of the interferogram were digitized at a sampling rate equivalent to a spectral width of 3156.8–0 cm^{-1}, and a low pass optical filter with a cutoff of ~2250 cm^{-1} was used to avoid aliasing. The averaged time-resolved double-sided interferograms were split into single side interferograms, to double the time resolution, and were Fourier transformed. Spectra were averaged between 78 and 94 s after photo-excitation to be used as reference to compute absorption difference spectra. The

resulting time-resolved difference spectra were subjected to singular value decomposition (SVD), as described.[53] Three SVD components were found to concentrate the signal and used to reconstruct the data with reduced noise. We performed global fitting combined with SVD in self-written routines running in Matlab.[54] The first two time-traces of highest significance were globally fitted to three exponentials to yield time constants of 37 ± 3 ms, 220 ± 70 ms, and 25 ± 3 s. These time constants are similar to those in solution experiments performed by flash-photolysis (Sineshchekov *et al.*[49] and our own unpublished results). Thus, in the hydrated films used for FT-IR spectroscopy, *Ca*ChR1 is immersed in sufficient water to exhibit "solution-like" dynamics.

III. RESULTS

A. Characterization of spectral changes in *Ca*ChR1 under continuous illumination

The light-induced IR difference spectrum of *Ca*ChR1 (Fig. 1) shows changes between the dark state and the intermediate state accumulated under photo-stationary conditions, as recently described.[48] Negative bands represent vibrations of the dark state of *Ca*ChR1 which are missing in the photo-accumulated intermediate state, and *vice versa* for the positive bands. The three negative bands in Fig. 1 at 1237 cm^{-1}, 1202 cm^{-1}, and 1163 cm^{-1} are assigned to C-C stretching vibrations of protonated all-*trans* retinal,[55] indicating that the photocycle in *Ca*ChR1 starts predominantly from the isomerization of the all-*trans* retinal, as in *Cr*ChR2[56,57] and in most microbial rhodopsins.[39] The IR intensity of the C-C stretching vibrations of the retinal is negligible unless the SB is protonated.[23,58] The absence of positive bands in this region (beside one weak band at 1176 cm^{-1}) confirms that an intermediate with deprotonated SB is predominantly accumulated. A detailed analysis of the retinal bands has recently been published.[48]

We performed time-resolved rapid-scan FT-IR experiments following a nanosecond laser pulse for excitation (Fig. 2(a)). The first recorded spectrum (6.5 ms after the laser pulse) lacks positive bands in the C-C stretching region of the retinal (1100-1300 cm^{-1}), a characteristic feature for intermediates with deprotonated SB.[23,58] Thus, the spectrum recorded at 6.5 ms after pulsed excitation represents an almost pure P_2^{380} spectrum (Fig. 2(b), top). P_2^{380} decay proceeds in a bi-exponential manner (with time constants of τ = 40 ms and 200 ms), which agrees well with previously reported time-resolved UV/Vis experiments.[49] From electrical current measurements of *Ca*ChR1 in HEK cells, it is known that the passive channel current last until approximately 40-50 ms, revealing the P_2^{380} intermediate as the conductive state of the channel.[49] After the P_2^{380} decay is completed, confirmed by the disappearance of all positive bands in the carboxylic region (1780–1700 cm^{-1}), a spectrum with a strong positive band in the C-C stretching region, at 1179 cm^{-1}, is observed (Fig. 2(b), bottom). This difference spectrum corresponds to a late intermediate with protonated SB, formed after the decay of P_2^{380}, which decays with τ = 25 s to the dark state. The presence of the negative bands at 1237, 1203, and 1161 cm^{-1} indicate that this intermediate (and the P_2^{380} intermediate) originates from the all-*trans* photocycle. Because photocurrents in *Ca*ChR1 cease in less than 100 ms,[49] but the vibrational changes persist for more than two orders of magnitude (Fig. 2(a)), we assign this intermediate to a P_4^{520} state.

Comparing the data from steady-state (Fig. 1) and time-resolved FT-IR spectroscopy (Fig. 2(a)), we conclude that the P_2^{380} intermediate is predominantly accumulated under continuous illumination of *Ca*ChR1, with little contributions from the P_4^{520} intermediate (see also Fig. S4 of the supplementary material[59]). Arguably, the similar absorption characteristics of the P_4^{520} and the dark state of *Ca*ChR1 leads to the excitation of the former under continuous illumination and, thus, to its immediate conversion to the initial dark state. Consequently, the long-lived P_2^{380} but not the P_4^{520} state, will accumulate. The accumulation of the P_2^{380} intermediate in *Ca*ChR1 under continuous illumination at room-temperature is in contrast to *Cr*ChR2, in which the desensitized state P_4^{480} is accumulated under these conditions.[56] Thus, *Ca*ChR1 is particularly well-suited to analyze for the first time internal waters of a ChR in the conductive state.

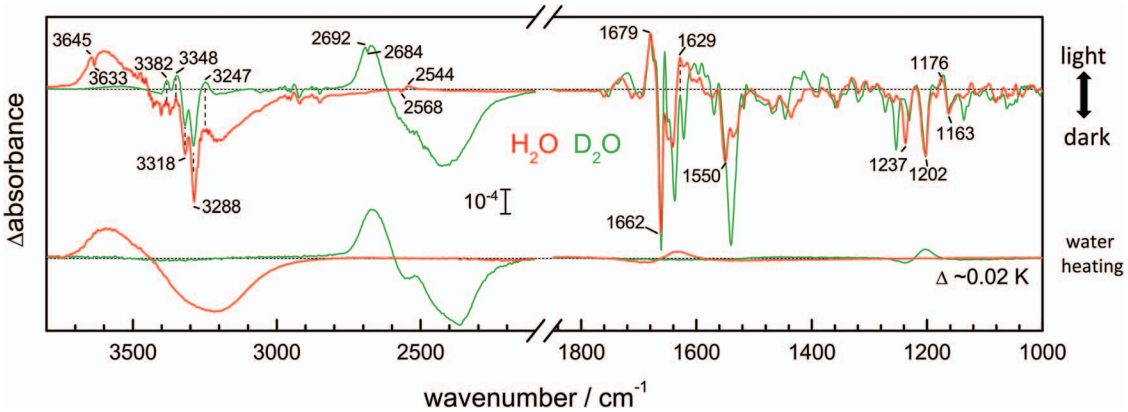

FIG. 1. (Top) Light-induced FT-IR difference spectra of *Ca*ChR1 in H_2O (red line) and D_2O (green line). Both spectra were recorded at 25 °C under illumination with an LED emitting at 505 nm. (Bottom) FT-IR difference spectrum of normal water (H_2O, red line) and heavy water (D_2O, green line) upon temperature change of 2 K (from 298 to 300 K), scaled to yield identical intensities in the water bands as those above. The scaling factor suggests a heating of ~0.02 K upon illumination of *Ca*ChR1.

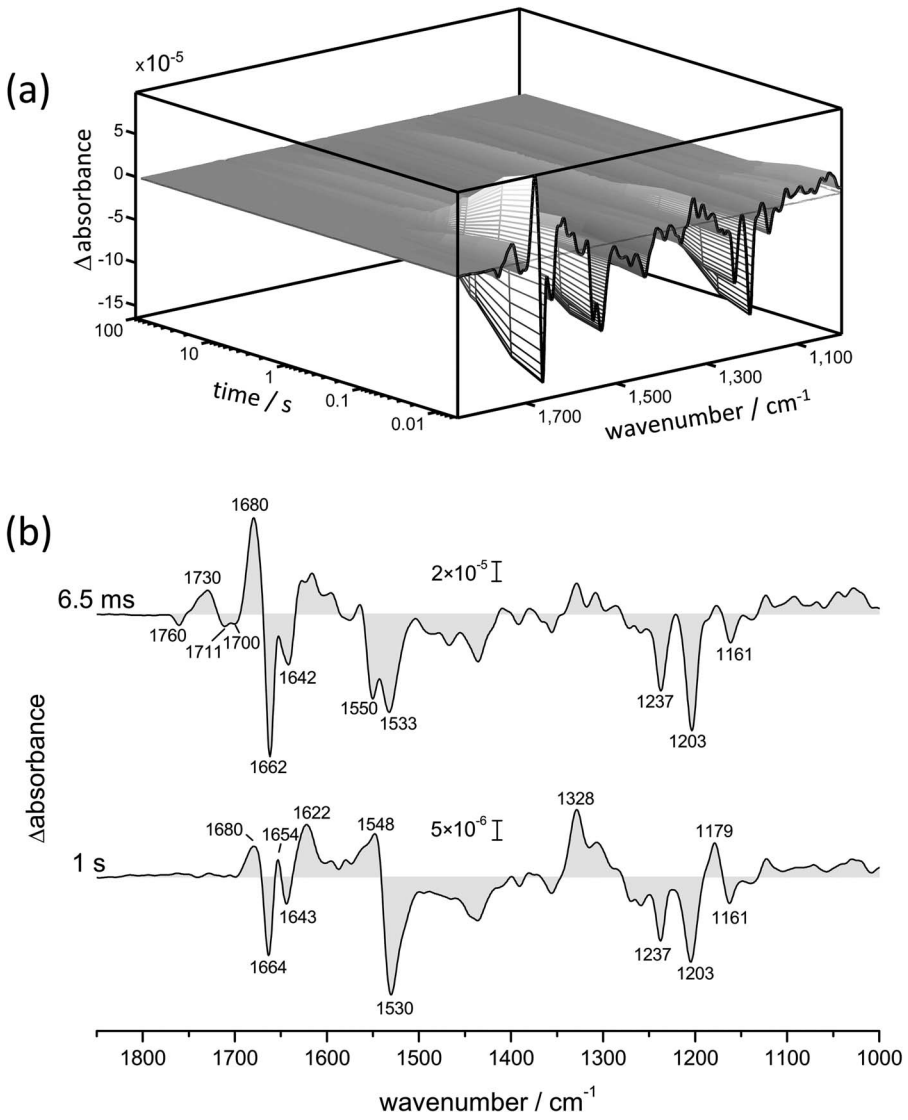

FIG. 2. Time-resolved rapid-scan FT-IR difference spectroscopy of *Ca*ChR1, extending from 6.5 ms to 94 s. (a) 3D representation of the experimental data, treated by singular value decomposition. (b) Spectra at 6.5 ms (P_2^{380} intermediate) and at 1 s (P_4^{520} intermediate) after pulsed laser excitation. Note that the different absorbance scales in the two spectra.

B. Spectral contributions from transient heating

The heat released after photo-excitation (internal conversion) slightly heats the solvent water in the sample.[34,60] As temperature rises, H-bonds become weakened on the average, leading to an upshift of O-H (and O-D) stretching frequencies. This results in a broad bilobic feature in the 3700–2900 cm^{-1} (2750–2150 cm^{-1}) region, better observed in the temperature-induced IR difference spectrum of pure water (bottom spectra in Fig. 1). Water heating also leads to minor spectral changes in the H-O-H (D-O-D) bending region at ∼1645 cm^{-1} (∼1210 cm^{-1}). As expected, we observe spectral changes in the O-H and O-D regions of the light-induced FT-IR spectra of *Ca*ChR1 similar in shape to those characteristic of water heating (Fig. 1). Based on its intensity, the calculated light-induced heating is very small, 0.02 K, but sufficient to lead to significant spectral distortions in the O-H and O-D stretching region that need to be corrected for, as described in Sec. II.

C. Changes in the peptide bond: Amide A, I, and II vibrations

Intense bands in typical regions for the peptide bond vibrations indicate notable alterations in the protein backbone structure between the ground state and the conductive P_2^{380} state of *Ca*ChR1 (Fig. 1). Specifically, the bands at 1679 (+), 1629 (+), and 1662 (−) cm^{-1} can be assigned to amide I vibrations, a coupled mode mostly contributed by the C=O stretching of the peptide bond.[61] The negative band at 1662 cm^{-1} appears at a wavenumber typical for transmembrane helices.[62,63] In agreement with this assignment, intense negative bands are resolved in the characteristic region for the amide A vibration (N-H stretching) of α-helices,[62,63] at 3318 cm^{-1} and 3288 cm^{-1}. The amide II vibration (N-H bending and C-N stretching) of α-helices appears typically around 1545–1540 cm^{-1} for α-helical transmembrane proteins.[63] Consequently, the negative band at 1550 cm^{-1} can be assigned to amide II vibrations, but partially also to

contributions from ethylenic (C = C) vibrations of the retinal chromophore, which were recently identified by resonance Raman spectroscopy.[48] The positive band at 1629 cm^{-1} is accompanied by a positive band at 3247 cm^{-1} (better resolved in the D_2O experiments, Fig. 1, top, green line) assigned to the amide I and amide A vibrations of β-strands, respectively.[64] The blue-shifted positive amide I band at 1679 cm^{-1}, as well as the amide A bands at 3382 and 3348 cm^{-1} (better resolved in D_2O experiments), are indicative for weakly H-bonded peptide C = O and N-H groups, often found in turns.[61] Overall, these bands indicate notable conformational changes in the protein backbone between the dark state and the P_2^{380} intermediate of *Ca*ChR1. Furthermore, we infer the amide groups involved in the conformational changes are mostly resistant to H/D exchange because the same bands are observed with similar intensity in the amide A region in H_2O and D_2O, most probable due to very stable intramolecular H-bonds.

D. Dangling O-H vibrations of active water molecules

The FT-IR difference spectrum of *Ca*ChR1 shows two narrow bands at 3645 and 3633 cm^{-1} (Fig. 1), this region is characteristic for weakly H-bonded O-H groups. To assess if these bands indeed originate form water molecules, we performed light-induced experiments after rehydrating the protein with $H_2{}^{18}O$ (Fig. 3(a), dashed lines). The exchange of $H_2{}^{16}O$ to $H_2{}^{18}O$ selectively increases the reduced mass associated to water vibrations, allowing to unambiguously identifying water bands by their vibrational downshift, excluding contributions from amino acid side chains (serine, threonine and tyrosine). We first computed a double difference spectrum between $H_2{}^{16}O$ and $H_2{}^{18}O$ (Fig. 3(b)), done to attenuate the spectral contributions from water heating without the need of performing a baseline correction. The result clearly shows the presence of two positive bands at 3648 and 3623 cm^{-1} and an about twice as intense negative band at 3634 cm^{-1}, indicating that both a positive (at ~3648 cm^{-1}) and the negative band (at ~3634 cm^{-1}) are sensitive to ^{18}O labeling of water.

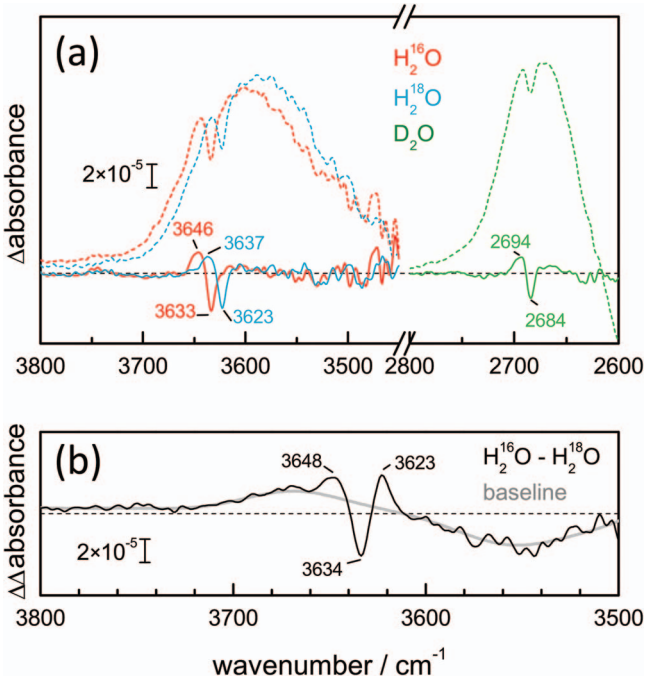

FIG. 3. Light induced FT-IR difference spectra of *Ca*ChR1 in the weakly H-bonded O-H and O-D regions (3800–2600 cm^{-1}) for various water isotopes. (a) Raw (dashed lines) and baseline corrected (continuous lines) spectra. (b) Double difference spectrum between experiments in $H_2{}^{16}O$ and in $H_2{}^{18}O$ (black line), including the baseline expected for bulk water upon $^{16}O/^{18}O$ exchange (gray line).

In an alternative procedure, the broad spectral contributions of water heating was digitally removed from the light-induced IR difference spectrum of *Ca*ChR1 as described in Sec. II (Fig. 3(a), continuous lines). In the O-H stretching region, we observed two narrow bands at 3646(+)/3633(−) cm^{-1} of 14 cm^{-1} and 7 cm^{-1} width, respectively. These two bands undergo a 9–11 cm^{-1} downshift to 3637(+)/3623(−) cm^{-1} in $H_2{}^{18}O$, without a change in their bandwidth. In D_2O, the two bands downshift by ~950 cm^{-1}, to 2694(+)/2684(−) cm^{-1}. The bands are narrower in D_2O, showing a width of 12 cm^{-1} and 6 cm^{-1}, respectively. The accuracy in the determination of the maximum of the above bands was higher than ± 0.3 cm^{-1} according to replicate experiments (see, for an example, Fig. S5 of the supplementary material[59]). The observed isotopic downshifts are in reasonable agreement with the shifts expected considering only the change in the reduced mass: 12 cm^{-1} for $H_2{}^{18}O$ and 990 cm^{-1} for D_2O. The intensities of the O-D bands are ~30% smaller than the corresponding O-H bands (Fig. 3(a)). This is in agreement with the ~30% smaller absorption coefficient of the O-D stretch than of the O-H stretch of water.[13,65] The narrower bands in D_2O are also coherent with the longer lifetime of the O-D stretch compared to the O-H stretch.[3] We conclude that *Ca*ChR1 contains a water molecule in the dark state with a weakly H-bonded O-H group. A water molecule with an even weaker H-bonded O-H group is present in the conductive P_2^{380} state.

E. Uncoupling experiments by isotopic dilution

The two O-H bonds of a water molecule represent coupled vibrators. In the extreme case of identical frequencies, e.g., for water in the gas phase, the O-H stretches couple into pure asymmetric and symmetric vibration modes at 3756 and 3657 cm^{-1} with a frequency gap of $2\gamma = 99$ cm^{-1} (where γ stands for the coupling constant). As the natural frequencies of the O-H stretches of water molecules in condensed phase exhibit larger differences, their coupling decreases. Therefore, the vibration frequency of a dangling O-H is indirectly sensitive to the frequency of the other O-H vibration in the same water molecule and, hence, to the strength of the H-bond at this second O-H group (see schematic Fig. 4).

Coupling-induced shifts can be determined by isotopic dilution experiments. We measured the light-induced FT-IR difference spectrum of *Ca*ChR1 in an H_2O/D_2O (1:1) mixture (Fig. 5(a), top). Under this condition, a dangling water will be an equimolar mixture of H_1-O-H_2, H_1-O-D_2, D_1-O-D_2, and D_1-O-H_2, where H_1 (D_1) represents the proton at the dangling O-H group (Fig. 4, left). The first two species give the coupled and uncoupled frequencies for the dangling O-H stretch and the last two the coupled and uncoupled frequencies for the dangling O-D stretch. For comparison, Fig. 5(a) (bottom)

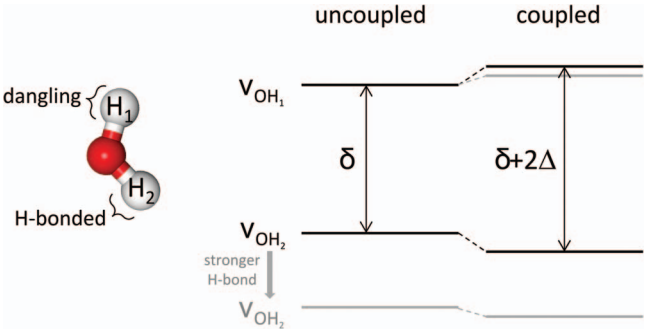

FIG. 4. (Left) Single water molecule with asymmetric O-H groups: Whereas the H_2-atom is H-bonded to an adequate acceptor, H_1 is dangling. (Right panel) Frequency levels of the O-H stretching of the water molecule. The natural (uncoupled) O-H frequencies differ by δ. Upon vibrational coupling, the frequencies up- and downshift by Δ, with a net increase in the frequency difference of 2Δ. Knowledge of Δ by uncoupling experiments allows inferring δ (see Eq. (1)). (Gray) A change in the natural frequency of O-H_2, induced by an altered H-bonding strength, affects the frequency of O-H_1 due to less efficient coupling.

reproduces the FT-IR difference spectrum for the fully coupled cases: in H_2O (100% H_1-O-H_2) and in D_2O (100% D_1-O-D_2).

The O-D stretch of the coupled (D_1-O-D_2) and uncoupled modes (D_1-O-H_2) are fully resolved in the H_2O/D_2O experiments. Positive bands appear at 2694 and 2678 cm^{-1} and negative bands at 2684 and 2673 cm^{-1}, i.e., the vibrational coupling upshifts the positive band by 16 cm^{-1} and the negative band by 11 cm^{-1} (Fig. 5(a) top). The coupled and uncoupled modes were not clearly resolved in the O-H region but

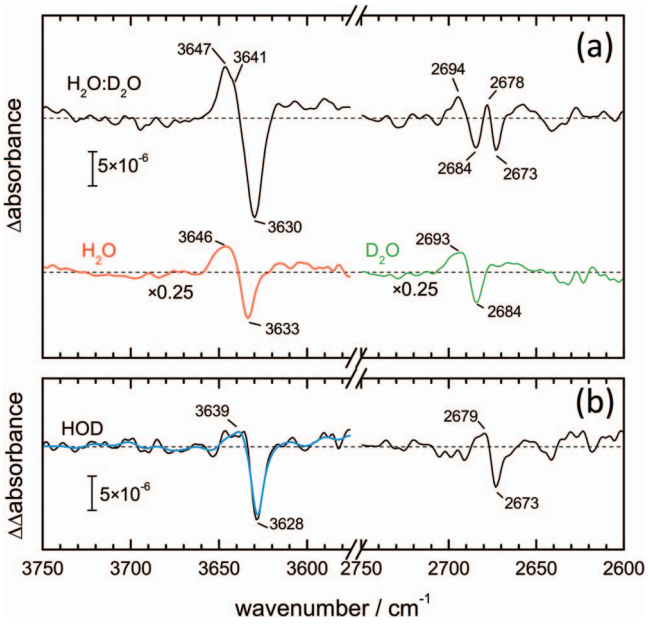

FIG. 5. Uncoupling experiments to observe the unperturbed O-H and O-D stretching vibration of water in *Ca*ChR1. (a) Difference spectrum when the sample was hydrated with a 1:1 mixture of H_2O:D_2O (black line), resulting in a mixture of 50% HOD, 25% HOH, and 25% DOD. Difference spectra for H_2O (red line) and D_2O (green line), were reproduced from Fig. 3 for comparison. (b) Calculated difference spectrum for HOD, displaying uncoupled O-H and O-D vibrations. The O-H region was smoothed for the accurate determination of the band maxima (blue line).

the positive band shows a shoulder and the negative band is broader, suggesting overlapping contributions.

The difference spectrum calculated for HOD, which represents an uncoupled difference spectrum, is shown in Fig. 5(b). This spectrum was obtained by proper subtraction of the spectra from the H_2O and D_2O experiments to that of the H_2O/D_2O mixture experiment, scaled to remove coupled spectral contributions. The fully uncoupled difference spectrum shows that the vibrational coupling upshift the positive band by ~7 cm^{-1} and the negative band by ~5 cm^{-1} in the O-H region. Note, the wavenumber shift upon uncoupling is roughly half for the O-H than for the O-D stretch. This difference is expected, given the slightly weaker intramolecular coupling constant in H_2O versus D_2O, but mostly due to the larger frequency discrepancy between the free O-H group and an average H-bonded O-H group for H_2O (~300 cm^{-1}) than for D_2O (~250 cm^{-1}).[19]

The observed shift upon uncoupling (Δ) is used to calculate the frequency difference between the natural frequencies of two coupled vibrations (δ) as given by the equation:[66]

$$\Delta = \sqrt{\left(\frac{\delta}{2}\right)^2 + \gamma^2} - \frac{\delta}{2}, \qquad (1)$$

where γ is the coupling strength constant. For D_2O in the gas phase the coupling strength constant is -58 cm^{-1}. *Ab initio* calculations for an isolated water molecule, with one dangling O-D and one H-bonded O-D (or O-H) group, estimated the coupling constant as -48 cm^{-1}.[67] Molecular dynamics simulations show that the value of γ is distributed in liquid D_2O.[19] It peaks at -40 cm^{-1} for bulk water and at -48 cm^{-1} for dangling water at the water-air interface. Taking $\gamma = -50 \pm 10$ cm^{-1} and applying the observed uncoupling shifts to Eq. (1), we can infer the natural O-D_2 frequency of the dangling water in the dark state of *Ca*ChR1 to be 2450 ± 100 cm^{-1} and in the P_2^{380} state to be 2530 ± 70 cm^{-1}. The uncoupled O-D frequency in liquid D_2O peaks at 2480 cm^{-1}, suggesting that the O-D_2 stretch of the dangling water is stronger H-bonded in the dark state and weaker H-bonded in the P_2^{380} intermediate of *Ca*ChR1 than in bulk water.

We performed similar calculations for the O-H stretch. For H_2O in the gas phase, the coupling strength constant is -49.5 cm^{-1}. Simulations suggested an average vibrational coupling of -27 cm^{-1} for liquid H_2O in the bulk phase.[68] *Ab initio* calculations for an isolated water molecule, with one dangling O-H and one H-bonded O-H (or O-D) group, provided a coupling constant of ~ -45 cm^{-1}.[67] Taking $\gamma = -40 \pm 10$ cm^{-1}, and considering the observed uncoupling shifts, we can infer the natural O-H_2 frequency of the dangling water in dark state *Ca*ChR1 to be 3300 ± 160 cm^{-1}, and in the P_2^{380} state 3440 ± 100 cm^{-1}. The uncoupled O-H frequency in liquid H_2O peaks at 3400 cm^{-1}, suggesting that the O-H_2 of the dangling water is in the dark state slightly stronger H-bonded and in the P_2^{380} intermediate slightly weaker H-bonded than in bulk water. These results agree well with those from the analysis of the O-D stretch (*vide supra*). Because of the smaller shifts and the smaller coupling constant, the uncertainties estimating the O-H stretching are larger than for the O-D stretching.

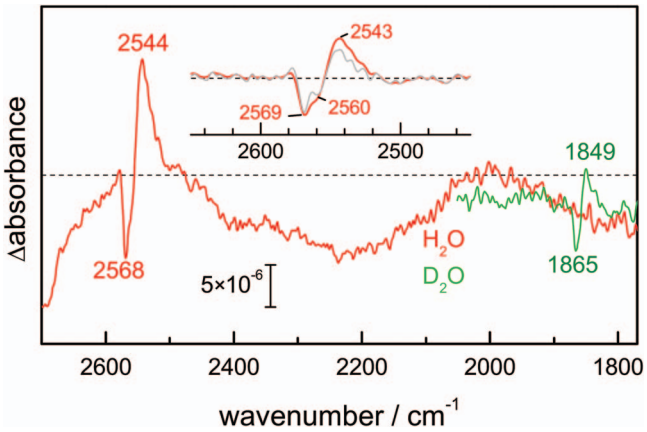

FIG. 6. Light-induced FT-IR difference spectra of *Ca*ChR1 in the S-H and S-D stretching region in H_2O (red) and D_2O (green). The inset shows the spectrum recorded in H_2O after baseline correction (red line) and band-narrowing by Fourier self-deconvolution (gray line).

F. Hydrogen-bonding changes of the thiol group of cysteine residues

The FT-IR difference spectrum of *Ca*ChR1 shows a pair of bands at 2568(−)/2544(+) cm^{-1} of a width of 10 and 18 cm^{-1}, respectively (Fig. 6, red line). This spectral region is highly specific in proteins for the S-H stretching vibration from the thiol group of cysteines.[69]

In D_2O, the bands shift to 1865(−)/1849(+) cm^{-1} (Fig. 6, green line). This 703/695 cm^{-1} downshift in D_2O is close to the theoretical downshift of 725 cm^{-1} expected from the increase in the reduced mass. The 2.5 times weaker intensity of the S-D band is in line with the 2.5–3 times reduced extinction coefficient of the S-D band compared to S-H.[70] Consequently, the sulfhydryl group of the probed cysteine (or cysteines) is fully susceptible to H/D exchange.

Likewise to the O-H stretch, the S-H stretch shifts to lower wavenumbers when it functions as H-bond donor. Methanethiol shows an S-H (S-D) stretch in the gas phase (non-hydrogen-bonded) at 2605 cm^{-1} (1893 cm^{-1}). The S-H stretching vibration of model compounds was investigated in various solvents of increased polarity.[71] The S-H was reported at 2585 cm^{-1} when non-hydrogen-bonded, while it was found at 2580–2575 cm^{-1} for weak H-bonded, at 2575–2560 cm^{-1} for moderate and at 2560–2525 cm^{-1} for strong H-bonded S-H groups.[71,72] Lower S-H stretching frequencies (down to 2477 cm^{-1}) have also been observed in proteins.[73] We should note that the H-bond acceptance by the sulfur atom has a minor effect in the S-H stretching frequency of model compounds, increasing the wavenumber frequency by less than ∼5 cm^{-1}.[71] This experimental observation challenges the conclusions from an homology model of *Cr*ChR2 refined by QM/MM simulations, suggesting that cysteine residues showing notable vibrational changes in the S-H stretch could be H-bonded only at the sulfur atom.[74] Therefore, the observed 24 cm^{-1} downshift of the S-H band between the dark state and the P_2^{380} state of *Ca*ChR1 must originate from an increase of the H-bond strength of the S-H group as a H-bond donor: from moderately to strongly H-bonded.

The negative band at 2568 cm^{-1} shows a shoulder, resolved after band-narrowing by Fourier deconvolution at 2560 cm^{-1} (Fig. 6, inset). This additional component, with half of the intensity compared to the main component at 2569 cm^{-1}, might be due to the presence of two rotamers with respect to the C-S torsion, known to lead at most to 10 cm^{-1} frequency shifts.[71,75] Indeed, similar subcomponents separated by 8 cm^{-1} have been observed in proteins and assigned to a mixture of cysteine rotamers before,[76,77] an assignment supported by simulations and structural data.[76,78] Still, the overlapping contribution of two cysteine side chains is an alternative explanation that cannot be discarded. Future mutational studies on *Ca*ChR1, where cysteines are selectively exchanged, will clarify this point. Based on the present results, we infer that at least one cysteine in *Ca*ChR1 shows a moderate H-bonded S-H group in the dark state (2568 cm^{-1}) which becomes strongly H-bonded in the conductive P_2^{380} intermediate (2544 cm^{-1}). This H-bonding change may report a conformational change in the opening of the channel.

IV. DISCUSSION

We have performed a vibrational analysis of the light-driven ion channel *Ca*ChR1, covering the X-H and X-D (X = O, S, N) region and specially focused on O-H (O-D) vibrations of active water molecules. Upon continuous illumination of *Ca*ChR1, a photocycle intermediate with deprotonated SB (P_2^{380}) is predominantly accumulated. The kinetics of the decay of this intermediate correlates with the decrease of the photocurrents.[49] Consequently, the observed spectral changes correspond to the formation of the conductive state of the channel that arises from the dark state.

A. Conformational changes of the protein backbone between the conductive and the dark state

The changes in the amide I region (1700–1620 cm^{-1}), associated to the formation of the P_2^{380} state from the dark state, are much larger than typically found in other microbial rhodopsins,[43] but comparable in intensity to those of *Cr*ChR2,[57] and the C1C2 chimera.[45] Nevertheless, bands in the structurally sensitive amide I region are significantly different in the conductive states of *Ca*ChR1 (P_2^{380}) and *Cr*ChR2 (late P_2^{390} and P_3^{520}), indicating differences in the structural changes that guide the opening of *Ca*ChR1 and *Cr*ChR2. We tentatively assigned bands in the amide I, II, and amide A regions of *Ca*ChR1 to changes in specific secondary structures. Briefly, the formation of the open state mainly involves changes in helices, but presumably also in β-strands and turns. Such light-induced changes in the tertiary structure of *Cr*ChR2 have been observed by EPR spectroscopy.[85]

B. Active water molecules in *Ca*ChR1

We assigned bands at 3646(+) and 3633(−) cm^{-1} to the O-H stretching of weakly H-bonded "dangling" water molecules in the P_2^{380} and in the dark state of *Ca*ChR1, respectively. Coupling-induced frequency shifts were measured

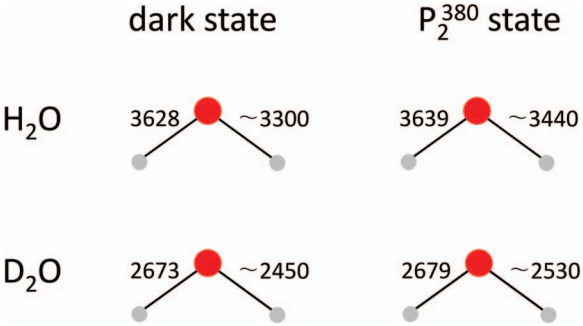

FIG. 7. Uncoupled O-H and O-D stretching frequencies of a water molecule in the dark and the conductive P_2^{380} state of *Ca*ChR1.

by isotopic uncoupling experiments. From these experiments, we inferred the frequency of two additional O-H stretches of water. The frequency shift between the coupled and uncoupled mode was then used to estimate the wavenumber separation of two O-H stretches in a water molecule. As a result, the natural (uncoupled) frequencies of four O-H (and O-D) stretches of water molecules was determined: in the dark state at 3628 and ~3300 cm^{-1} (2673 and ~2450 cm^{-1}) and in the P_2^{380} state at 3639 and ~3440 cm^{-1} (2679 and ~2530 cm^{-1}), as visually summarized in Fig. 7.

The frequencies of the O-H (O-D) stretches, at 3300 and 3440 cm^{-1} (2450 and 2530 cm^{-1}), appear in a region that challenges their direct experimental observation due to overlapping spectral components, water heating artifacts, and band broadening associated to lower O-H stretching frequencies. Therefore, the present approach using uncoupling isotopic experiments can be useful to detect medium/strongly H-bonded O-H groups of water when the other O-H group is weakly H-bonded. The error in the wavenumber of the coupled O-H (O-D) stretches is around ± 130 cm^{-1} (± 85 cm^{-1}), caused by the relative large uncertainty in the value of the vibrational coupling constant, an issue that could be improved by suitable theoretical studies. The determination of the uncoupling shifts, the main source of experimental error, is significantly smaller. A generous estimate of the error in the uncoupling shifts of ± 1 cm^{-1} leads to an error of around ± 60 cm^{-1} (± 20 cm^{-1}) in the coupled O-H (O-D) frequency. The error is larger for the O-H than for the O-D stretch, due to the smaller shifts in the former. We should note that the same approach used here was performed before to characterize the vibration frequency of the two O-H groups of water molecules at the water-air interface.[19] For proteins, coupled and uncoupled O-H vibrations of dangling waters have only been detected in the S1 and in the S2 states of photosystem II.[33] These shifts were quantitatively analyzed later by a different group, with some inconsistent results between the O-H and O-D data.[67]

Applying known empirical correlations between the H-bond energy from the O-H stretch frequency,[7] and taking 3706 cm^{-1} as the O-H stretch of non-hydrogen-bonded water, we estimate the H-bonding energies of the O-H stretches of water: 3628 cm^{-1} → 11.6 kJ/mol and 3300 cm^{-1} → 26.2 kJ/mol for the dark state, as well as 3639 cm^{-1} → 10.7 kJ/mol and 3440 cm^{-1} → 21.2 kJ/mol for the P_2^{380} state. Thus, the energy, which is stored in the H-bonds of dangling waters, is reduced by about 6 kJ/mol upon formation of the conductive state.

The two bands from water molecules observed upon formation of the P_2^{380} intermediate of *Ca*ChR1, at 3646(+) and 3634(−) cm^{-1} (Fig. 3), are reminiscent to two water bands at 3671(+) and 3643(−) cm^{-1} resolved in the M intermediate of BR, an intermediate as P_2^{380} with a deprotonated SB. In BR, a dangling water with an O-H (O-D) vibration at 3643 cm^{-1} (2690 cm^{-1}) in the ground state was assigned by experiments and calculations to the crystallographic water molecule W401.[27] This water molecule is H-bonded at its second O-H group to D85, forming part of the pentagonal arrangement around the protonated SB. This pentagonal H-bonded network is built on three water molecules and the ionized side chains of R82, D85, and D212. The O-D frequency of the H-bonded O-D group of W401 was determined in experiments to be at 2323 cm^{-1},[27] while the O-H frequency was estimated by QM/MM calculations to be at 3325 cm^{-1},[79] both indicating a medium/strong H-bond. A water molecule near the SB was also resolved in the X-ray structure of the C1C2 chimera of ChR (W619, see Fig. 8).[44] In an FT-IR study on the C1C2 chimera, a water molecule with the O-D stretch at 2378 cm^{-1} was assigned by its sensitivity to site-directed mutations to a water molecule H-bonded to D292 in the dark state,[45] a residue equivalent to D212 in BR. In the dark state of *Ca*ChR1, we estimate the O-H (O-D) frequency of the H-bonded O-H group of a dangling water at 3300 cm^{-1} (2450 cm^{-1}), only slightly upshifted in respect to water W401 of BR and to the above discussed water molecule of the C1C2 chimera.[45] Thus, in homology with BR and C1C2, we suggest that this water molecule might take part, together with R166, E169, and D299 (see Fig. 8) and additional water molecules, in the H-bonding network of *Ca*ChR1 stabilizing the protonated SB. This suggestion goes in line with the increased bandwidth of the C=N stretch of the SB in H_2O than in D_2O, as was observed by resonance Raman spectroscopy.[48] This effect is likely due to a more efficient vibrational relaxation of the C=N stretch due to efficient energy transfer to the bending vibration of H_2O, both with similar vibration frequency, indicating that water is directly H-bonded or at least in very close proximity to the SB.[48] In BR the dangling O-H vibration at 3643 cm^{-1} in the dark state is missing in the L intermediate, i.e., prior to the proton transfer from the protonated SB to D85,[24,25] indicating a reorganization of H-bonds of water molecules that could be critical for this proton transfer to occur. A similar role for the water molecules around the SB can be envisaged in ChRs.

In BR, another dangling water is formed upon deprotonation of the SB, characterized by an O-H stretch at 3671 cm^{-1}.[24,25] This water fills a hydrophobic cavity located in the cytoplasmic transmembrane part of BR. It has been suggested that this water molecule assists, along with two other water molecules, the reprotonation of the SB by D96.[24,36] Thus, in BR two dangling waters could be localized at atomic resolution and were shown to be involved in H-bonding networks inside the protein. This H-bonding network is crucial for internal proton transfer reactions, and, thus, for the proton-pump mechanism of BR. In *Cr*ChR2, the SB proton donor

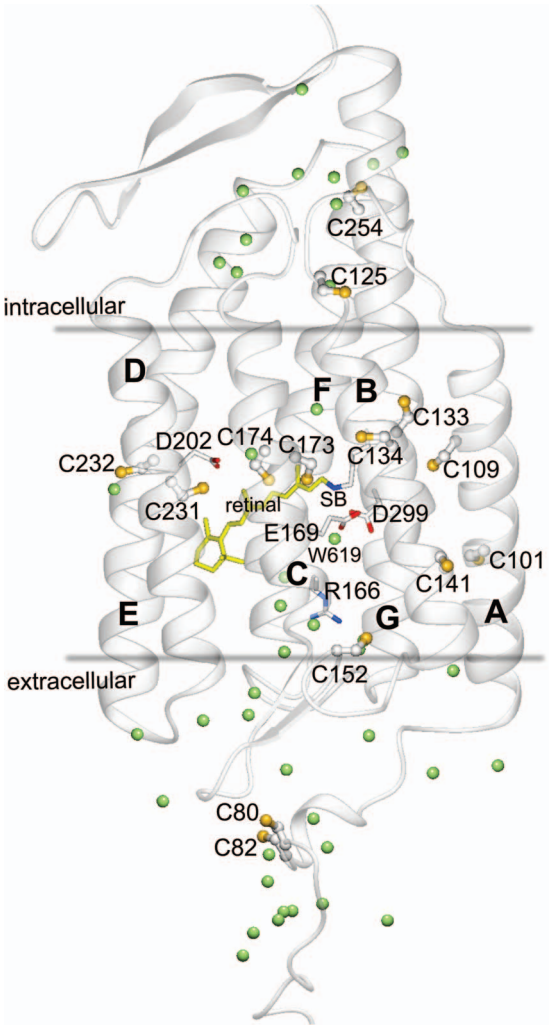

FIG. 8. Structural model of *Ca*ChR1 derived by homology modeling and build by the SWISS-MODEL server[81] using the C1C2 structure as template (pdb: 3UG9).[44] The gray horizontal lines indicate the membrane part of the channel. The retinal chromophore is located in the middle of the membrane (yellow sticks) and bound via a Schiff base, SB (blue), linkage to the apoprotein. All cysteine residues of *Ca*ChR1 are highlighted, as well as amino acids that are potentially involved in the SB counterion complex (R166, E169, D299) and the putative SB proton donor (D202). Water molecules resolved in the C1C2 structure are displayed as green spheres, including W619 near E169 and D299. The molecular graph was generated with the BALLView software.[82]

is D156 (D115 in BR). Although the X-ray structure of the C1C2 chimera does not display a water molecule close to the equivalent location,[44] MD simulations indicate the presence of a nearby water molecule.[80] Therefore, it is tempting to suggest that the dangling water observed upon formation of the P_2^{380} intermediate in *Ca*ChR1 is located in the cytoplasmic transmembrane part to assist reprotonation of the SB. To determine their location and to determine if the dangling waters in *Ca*ChR1 have a similar role as in BR, a joint effort of site-directed mutagenesis, IR spectroscopy, high-resolution crystallography, and simulations is required.

C. Hydrogen-bonding changes in the side chain of internal cysteines

A frequency downshift of the vibrational band of the S-H stretching was observed upon illumination of *Ca*ChR1 (Fig. 6) with bands resolved at 2569(−), 2560(−), and 2543(+) cm^{-1}, suggesting H-bonding changes in one or more cysteine side chains upon formation of the conductive state. Changes in the S-H stretching vibration have been reported for a few retinal proteins before, predominantly at cryogenic temperatures. For instance, *Neurospora* rhodopsin showed bands at 2573(+), 2564(+), and 2560(−) cm^{-1},[46] *Anabaena* sensory rhodopsin (ASR) at 2547(−) and 2538(+) cm^{-1},[83] and the C1C2 chimera bands at 2596(+) and 2577(−) cm^{-1} (Ref. 45) upon illumination at 77 K. At room temperature, ASR displayed bands at 2564(−), 2554(+), and 2544(−) cm^{-1}.[84] Thus, the S-H bands of *Ca*ChR1 appear in a frequency range similar to S-H bands of *Neurospora* and ASR.

*Ca*ChR1 contains as many as 14 cysteines (Fig. 8), which renders the assignment difficult. The sulfhydryl group of the cysteine side chain is highly polarizable with a transition dipole moment in the S-H stretch that is strongly dependent on its environment.[72,85] For instance, the extinction coefficient of the S-H stretch in water is very weak ($\sim$ 5 $M^{-1}\,cm^{-1}$),[72,85] making solvent exposed cysteine residues practically undetectable by IR spectroscopy.[86] Instead, an increase in the extinction coefficient by a factor of $\sim$30 is observed when the S-H is buried in the protein,[86] suggesting that the resolved S-H in *Ca*ChR1 is unlikely to originate from a cysteine residues in the loop region (C80, C82, C125, C152, and C254). This rationale reduces the likely candidates to the nine transmembrane cysteines (see Fig. 8), namely, C101 and C109 on helix A, C133, C134, and C141 on helix B, C173 and C174 on helix C, and C231 and C232 on helix E. Below, we will discuss possible candidates but mutational work will be required for a definite band assignment.

There are two most common ways how thiol groups form H-bonds, either intrahelical with the oxygen atom of the backbone chain of the same helix or interhelical with a side chain of another helix.[74,87] Consequently, a change in H-bonding strength of a cysteine side chain might originate either by a change in the pitch of the helix in the case of an intrahelical H-bond or a change in the relative orientation of two helices in the case of an interhelical H-bond. For *Cr*ChR2, it has been shown that the photocycle is associated with the movement of transmembrane helices, predominantly of helices B and F.[88] Because helix F of *Ca*ChR1 lacks cysteine residues, the cysteine residues in helix B (C133, C134, and C141) are prime candidates to undergo a measurable change in their S-H stretch frequency as a result of the structural changes.

Archetypical microbial rhodopsins either lack native cysteine residues (e.g., bacteriorhodopsin) or contain only a few. *Anabaena* sensory rhodopsin (ASR) contains three cysteine residues, two of them changing their S-H vibration frequency in the photocycle and assigned by site-directed mutagenesis to C137 (helix E) and C203 (helix G).[84] The first cysteine, C137, is conserved in *Cr*ChR1 (C222) and *Cr*ChR2 (C183), and in the derived C1C2 chimera (C222).[44,74] The above cysteine is not conserved in *Ca*ChR1 (T229), but two cysteine residues are present nearby in helix E (C231 and C232). Thus, these two residues are prime candidates to change their S-H stretches during the photocycle of *Ca*ChR1, as well. The second "active" cysteine of ASR, C203, is not conserved

in *Cr*ChRs (A289 in *Cr*ChR1 and T250 in *Cr*ChR2) nor in *Ca*ChR1 (S296).

An H-bond between the cysteine C128 and the aspartic acid D156, known as the DC gate, was shown to build a structural motif that influences the kinetics of channel closure in *Cr*ChR2.[43,89] These two residues correspond to C174 and D202 in *Ca*ChR1 (Fig. 8). D156 in *Cr*ChR2 was further identified as the proton donor to the SB and the role of the DC gate was proposed to raise the pKa of D156 to stabilize the protonated form in the dark state.[90] The crystal structure of the dark state of the C1C2 chimera did not support an H-bond between the equivalent residues C167 and D195 (C1C2 numbering),[44] a controversial result challenging the molecular nature of the DC gate.[43,89] Nevertheless, FT-IR measurements at 77 K on the C1C2 chimera detected S-H difference bands between the dark state and the P_1 intermediate, tentatively assigned to C167.[45] Given their frequency, 2596(+)/2577(−) cm^{-1}, it was concluded that the S-H group is not H-bonded in the P_1 state but weakly H-bonded in the dark state. The latter result contradicts the X-ray structural model of the dark state C1C2 chimera. In *Cr*ChR2, bands in the S-H region were detected in the P_1^{500} and the P_4^{480} state.[91] Upon the D156E mutation a 4 cm^{-1} downshift was observed for the S-H bands in the P_4^{480} intermediate, but not in the P_1^{500} intermediate. This result indicates that the S-H bands in the P_4^{480} intermediate arise from C128, at least partially, which is close to D156. Following these results, the bands in the S-H stretch region of *Ca*ChR1 might originate from the equivalent residue, C174, at least in part.

V. CONCLUSIONS

We reported for the first time on vibrational changes in the S-H stretching of the conductive state of any ChR. The formation of the P_2^{380} state of *Ca*ChR1 leads to stronger H-bonding of a cysteine residue(s). If the S-H vibration is due to C174 (equivalent to C128 in *Cr*ChR2) or to cysteine residues of helix B (C133, C134, and C141) or helix E (C231 and C232), will be addressed in site-directed mutagenesis experiments.

We also performed a detailed vibrational analysis of the four O-H (and O-D) stretching vibrations of water molecules in *Ca*ChR1, two in the dark and two in P_2^{380} state. This is the first time that changes in the O-H stretching vibration of water molecules have been characterized upon the formation of the conductive state of any ChR. Similar vibrational changes of water molecules were observed previously in BR, and shown to be involved in proton transfer reactions essential for the proton-pumping mechanism of this protein. Whether a similar role can be assigned to the detected water molecules in *Ca*ChR1, will be elucidated in the future. Such studies are underway.

ACKNOWLEDGMENTS

We thank D. Heinrich, K. Hoffmann, J. Wonneberg, and I. Wallat for excellent technical assistance. V.M. is a recipient of a grant from the Leibniz Graduate School of Molecular Biophysics. Financial support came from the Deutsche Forschungsgemeinschaft (SFB 1078, projects B3 to J.H. and B4 to R.S.).

[1] P. Ball, Nature (London) **452**(7185), 291 (2008).
[2] P. Ball, Chem. Rev. **108**(1), 74 (2008).
[3] H. J. Bakker and J. L. Skinner, Chem. Rev. **110**(3), 1498 (2010).
[4] A. K. Soper and C. J. Benmore, Phys. Rev. Lett. **101**(6), 065502 (2008).
[5] P. Wernet, D. Nordlund, U. Bergmann, M. Cavalleri, M. Odelius, H. Ogasawara, L. A. Naslund, T. K. Hirsch, L. Ojamae, P. Glatzel, L. G. Pettersson, and A. Nilsson, Science **304**(5673), 995 (2004); J. J. Max and C. Chapados, J. Chem. Phys. **134**(16), 164502 (2011); **133**(16), 164509 (2010).
[6] K. Nakamoto, M. Margoshes, and R. E. Rundle, J. Am. Chem. Soc. **77**(24), 6480 (1955).
[7] M. Rozenberg, A. Loewenschuss, and Y. Marcus, Phys. Chem. Chem. Phys. **2**(12), 2699 (2000).
[8] C. P. Lawrence and J. L. Skinner, J. Chem. Phys. **118**(1), 264 (2003); C. J. Fecko, J. D. Eaves, J. J. Loparo, A. Tokmakoff, and P. L. Geissler, Science **301**(5640), 1698 (2003).
[9] W. Kulig and N. Agmon, Nat. Chem. **5**(1), 29 (2013).
[10] D. N. Glew and N. S. Rath, Can. J. Chem. **49**(6), 837 (1971).
[11] A. V. Iogansen, Spectrochim. Acta A **55**(7-8), 1585 (1999).
[12] E. T. J. Nibbering and T. Elsaesser, Chem. Rev. **104**(4), 1887 (2004).
[13] J. E. Bertie and M. K. Ahmed, J. Phys. Chem. **93**, 2210 (1989).
[14] J. D. Eaves, J. J. Loparo, C. J. Fecko, S. T. Roberts, A. Tokmakoff, and P. L. Geissler, Proc. Natl. Acad. Sci. U.S.A. **102**(37), 13019 (2005).
[15] J. Lindner, P. Vohringer, M. S. Pshenichnikov, D. Cringus, D. A. Wiersma, and M. Mostovoy, Chem. Phys. Lett. **421**(4-6), 329 (2006).
[16] D. Marx, Science **303**(5658), 634 (2004).
[17] Q. Du, R. Superfine, E. Freysz, and Y. R. Shen, Phys. Rev. Lett. **70**(15), 2313 (1993).
[18] C. S. Hsieh, R. K. Campen, M. Okuno, E. H. Backus, Y. Nagata, and M. Bonn, Proc. Natl. Acad. Sci. U.S.A. **110**(47), 18780 (2013).
[19] I. V. Stiopkin, C. Weeraman, P. A. Pieniazek, F. Y. Shalhout, J. L. Skinner, and A. V. Benderskii, Nature (London) **474**(7350), 192 (2011).
[20] J. W. Shin, N. I. Hammer, E. G. Diken, M. A. Johnson, R. S. Walters, T. D. Jaeger, M. A. Duncan, R. A. Christie, and K. D. Jordan, Science **304**(5674), 1137 (2004); M. Miyazaki, A. Fujii, T. Ebata, and N. Mikami, *ibid.* **304**(5674), 1134 (2004).
[21] J. M. Headrick, E. G. Diken, R. S. Walters, N. I. Hammer, R. A. Christie, J. Cui, E. M. Myshakin, M. A. Duncan, M. A. Johnson, and K. D. Jordan, Science **308**(5729), 1765 (2005).
[22] Y. Umena, K. Kawakami, J. R. Shen, and N. Kamiya, Nature (London) **473**(7345), 55 (2011); H. Luecke, B. Schobert, H. T. Richter, J. P. Cartailler, and J. K. Lanyi, J. Mol. Biol. **291**(4), 899 (1999); T. Tiefenbrunn, W. Liu, Y. Chen, V. Katritch, C. D. Stout, J. A. Fee, and V. Cherezov, PLoS One **6**(7), e22348 (2011).
[23] A. Maeda, Isr. J. Chem. **35**, 387 (1995).
[24] H. Kandori, Biochim. Biophys. Acta **1460**(1), 177 (2000).
[25] A. Maeda, Biochemistry (Mosc.) **66**(11), 1256 (2001).
[26] H. Kandori and Y. Shichida, J. Am. Chem. Soc. **122**(47), 11745 (2000).
[27] M. Shibata and H. Kandori, Biochemistry **44**(20), 7406 (2005).
[28] H. Kandori, Y. Furutani, K. Shimono, Y. Shichida, and N. Kamo, Biochemistry **40**(51), 15693 (2001).
[29] Y. Furutani and H. Kandori, Biochim. Biophys. Acta **1837**(5), 598 (2014).
[30] Y. S. Chon, H. Kandori, J. Sasaki, J. K. Lanyi, R. Needleman, and A. Maeda, Biochemistry **38**(29), 9449 (1999); T. Nagata, A. Terakita, H. Kandori, D. Kojima, Y. Shichida, and A. Maeda, *ibid.* **36**(20), 6164 (1997).
[31] T. Iwata, M. L. Paddock, M. Y. Okamura, and H. Kandori, Biochemistry **48**(6), 1220 (2009); H. Kandori, T. Iwata, J. Hendriks, A. Maeda, and K. J. Hellingwerf, *ibid.* **39**(27), 7902 (2000).
[32] A. Marechal and P. R. Rich, Proc. Natl. Acad. Sci. U.S.A. **108**(21), 8634 (2011); T. Noguchi and M. Sugiura, Biochemistry **41**(52), 15706 (2002); Y. Furutani, K. Fujiwara, T. Kimura, T. Kikukawa, M. Demura, and H. Kandori, J. Phys. Chem. Lett. **3**, 2964 (2012); V. B. Bergo, E. N. Spudich, J. L. Spudich, and K. J. Rothschild, Biochemistry **48**(5), 811 (2009); J. E. Morgan, A. S. Vakkasoglu, R. B. Gennis, and A. Maeda, *ibid.* **46**(10), 2787 (2007).
[33] T. Noguchi and M. Sugiura, Biochemistry **39**(36), 10943 (2000).
[34] V. A. Lórenz-Fonfría, Y. Furutani, and H. Kandori, Biochemistry **47**(13), 4071 (2008).
[35] H. Suzuki, M. Sugiura, and T. Noguchi, Biochemistry **47**(42), 11024 (2008).
[36] F. Garczarek and K. Gerwert, Nature (London) **439**(7072), 109 (2006).

[37]M. Grote, M. Engelhard, and P. Hegemann, Biochim. Biophys. Acta **1837**(5), 533 (2014); J. L. Spudich, O. A. Sineshchekov, and E. G. Govorunova, *ibid.* **1837**(5), 546 (2014).
[38]G. Nagel, D. Ollig, M. Fuhrmann, S. Kateriya, A. M. Musti, E. Bamberg, and P. Hegemann, Science **296**(5577), 2395 (2002); G. Nagel, T. Szellas, W. Huhn, S. Kateriya, N. Adeishvili, P. Berthold, D. Ollig, P. Hegemann, and E. Bamberg, Proc. Natl. Acad. Sci U.S.A. **100**(24), 13940 (2003).
[39]J. L. Spudich, C. S. Yang, K. H. Jung, and E. N. Spudich, Annu. Rev. Cell. Dev. Biol. **16**, 365 (2000); O. P. Ernst, D. T. Lodowski, M. Elstner, P. Hegemann, L. S. Brown, and H. Kandori, Chem. Rev. **114**(1), 126 (2014).
[40]P. Hegemann, Annu. Rev. Plant Biol. **59**, 167 (2008).
[41]L. Fenno, O. Yizhar, and K. Deisseroth, Annu. Rev. Neurosci. **34**, 389 (2011).
[42]K. Stehfest and P. Hegemann, ChemPhysChem **11**(6), 1120 (2010).
[43]V. A. Lórenz-Fonfría and J. Heberle, Biochim. Biophys. Acta **1837**(5), 626 (2014).
[44]H. E. Kato, F. Zhang, O. Yizhar, C. Ramakrishnan, T. Nishizawa, K. Hirata, J. Ito, Y. Aita, T. Tsukazaki, S. Hayashi, P. Hegemann, A. D. Maturana, R. Ishitani, K. Deisseroth, and O. Nureki, Nature (London) **482**(7385), 369 (2012).
[45]S. Ito, H. E. Kato, R. Taniguchi, T. Iwata, O. Nureki, and H. Kandori, J. Am. Chem. Soc. **136**(9), 3475 (2014).
[46]Y. Furutani, A. G. Bezerra, Jr., S. Waschuk, M. Sumii, L. S. Brown, and H. Kandori, Biochemistry **43**(30), 9636 (2004).
[47]S. Y. Hou, E. G. Govorunova, M. Ntefidou, C. E. Lane, E. N. Spudich, O. A. Sineshchekov, and J. L. Spudich, Photochem. Photobiol. **88**(1), 119 (2012).
[48]V. Muders, S. Kerruth, V. A. Lórenz-Fonfría, C. Bamann, J. Heberle, and R. Schlesinger, FEBS Lett. **588**, 2301 (2014).
[49]O. A. Sineshchekov, E. G. Govorunova, J. Wang, H. Li, and J. L. Spudich, Biophys. J. **104**(4), 807 (2013).
[50]T. Noguchi and M. Sugiura, Biochemistry **41**(7), 2322 (2002).
[51]E. Goormaghtigh, V. Raussens, and J. M. Ruysschaert, Biochim. Biophys. Acta **1422**(2), 105 (1999).
[52]J. E. Bertie and Z. D. Lan, Appl. Spectrosc. **50**(8), 1047 (1996).
[53]V. A. Lórenz-Fonfría and H. Kandori, J. Am. Chem. Soc. **131**(16), 5891 (2009).
[54]V. A. Lórenz-Fonfría and H. Kandori, Appl. Spectrosc. **61**(4), 428 (2007).
[55]S. O. Smith, J. Lugtenburg, and R. A. Mathies, J. Membr. Biol. **85**(2), 95 (1985).
[56]E. Ritter, K. Stehfest, A. Berndt, P. Hegemann, and F. J. Bartl, J. Biol. Chem. **283**(50), 35033 (2008).
[57]I. Radu, C. Bamann, M. Nack, G. Nagel, E. Bamberg, and J. Heberle, J. Am. Chem. Soc. **131**(21), 7313 (2009).
[58]K. Gerwert and F. Siebert, EMBO J. **5**(4), 805 (1986).
[59]See supplementary material at http://dx.doi.org/10.1063/1.4895796 for visible absorption spectra of *Ca*ChR1 and *Cr*ChR2 (Fig. S1), for IR absorption spectra of *Ca*ChR1 hydrated with H_2O and D_2O (Fig. S2), for the calculated effective penetration depth used to correct the attenuated total reflection experiments of water (Fig. S3), for FT-IR steady-state spectra of *Ca*ChR1 compared with rapid-scan spectra at two different times (Fig. S4), and for FT-IR steady-state spectra of *Ca*ChR1 showing the reproducibility of the band maxima for "dangling" O-H stretches of water (Fig. S5).
[60]F. Garczarek, J. Wang, M. A. El-Sayed, and K. Gerwert, Biophys. J. **87**(4), 2676 (2004).
[61]S. Krimm and J. Bandekar, Adv. Protein Chem. **38**, 181 (1986).
[62]N. Dave, V. A. Lórenz-Fonfría, G. Leblanc, and E. Padrós, Biophys. J. **94**(9), 3659 (2008).
[63]E. Goormaghtigh, V. Cabiaux, and J. M. Ruysschaert, Subcell. Biochem. **23**, 405 (1994).
[64]E. Goormaghtigh, V. Cabiaux, and J. M. Ruysschaert, Subcell. Biochem. **23**, 329 (1994).
[65]J. J. Max and C. Chapados, J. Chem. Phys. **131**(18), 184505 (2009).
[66]I. R. Levine, *Quantum Chemistry*, 5th ed. (Prentice-Hall, New Jersey, 2000).
[67]G. Fischer and T. Wydrzynski, J. Phys. Chem. B **105**(51), 12894 (2001).
[68]B. M. Auer and J. L. Skinner, J. Chem. Phys. **128**(22), 224511 (2008).
[69]A. Barth, Prog. Biophys. Mol. Biol. **74**(3–5), 141 (2000).
[70]T. Noguchi, Y. Fukami, H. Oh-oka, and Y. Inoue, Biochemistry **36**(40), 12329 (1997).
[71]H. M. Li and G. J. Thomas, J. Am. Chem. Soc. **113**(2), 456 (1991).
[72]G. H. Bare, J. O. Alben, and P. A. Bromberg, Biochemistry **14**(8), 1578 (1975).
[73]H. Kandori, N. Kinoshita, Y. Shichida, A. Maeda, R. Needleman, and J. K. Lanyi, J. Am. Chem. Soc. **120**(23), 5828 (1998).
[74]H. C. Watanabe, K. Welke, F. Schneider, S. Tsunoda, F. Zhang, K. Deisseroth, P. Hegemann, and M. Elstner, J. Biol. Chem. **287**(10), 7456 (2012).
[75]H. M. Li, C. J. Wurrey, and G. J. Thomas, J. Am. Chem. Soc. **114**(19), 7463 (1992).
[76]Y. Sato, M. Nabeno, T. Iwata, S. Tokutomi, M. Sakurai, and H. Kandori, Biochemistry **46**(36), 10258 (2007).
[77]T. Bednarz, A. Losi, W. Gartner, P. Hegemann, and J. Heberle, Photochem. Photobiol. Sci. **3**(6), 575 (2004).
[78]R. Fedorov, I. Schlichting, E. Hartmann, T. Domratcheva, M. Fuhrmann, and P. Hegemann, Biophys. J. **84**(4), 2474 (2003).
[79]M. Baer, G. Mathias, I. F. W. Kuo, D. J. Tobias, C. J. Mundy, and D. Marx, ChemPhysChem **9**(18), 2703 (2008).
[80]H. C. Watanabe, K. Welke, D. J. Sindhikara, P. Hegemann, and M. Elstner, J. Mol. Biol. **425**(10), 1795 (2013).
[81]F. Kiefer, K. Arnold, M. Kunzli, L. Bordoli, and T. Schwede, Nucl. Acids Res. **37**, D387 (2009); K. Arnold, L. Bordoli, J. Kopp, and T. Schwede, Bioinformatics **22**(2), 195 (2006); N. Guex, M. C. Peitsch, and T. Schwede, Electrophoresis **30**(Suppl 1), S162 (2009).
[82]A. Moll, A. Hildebrandt, H. P. Lenhof, and O. Kohlbacher, Bioinformatics **22**(3), 365 (2006); J. Comput. Aided Mol. Des. **19**(11), 791 (2005).
[83]A. Kawanabe, Y. Furutani, K. H. Jung, and H. Kandori, Biochemistry **45**(14), 4362 (2006).
[84]V. B. Bergo, M. Ntefidou, V. D. Trivedi, J. J. Amsden, J. M. Kralj, K. J. Rothschild, and J. L. Spudich, J. Biol. Chem. **281**(22), 15208 (2006).
[85]P. P. Moh, F. G. Fiamingo, and J. O. Alben, Biochemistry **26**(19), 6243 (1987).
[86]M. Koziński, S. Garrett-Roe, and P. Hamm, J. Phys. Chem. B **112**(25), 7645 (2008).
[87]P. Zhou, F. Tian, F. Lv, and Z. Shang, Proteins **76**(1), 151 (2009).
[88]N. Krause, C. Engelhard, J. Heberle, R. Schlesinger, and R. Bittl, FEBS Lett. **587**(20), 3309 (2013); T. Sattig, C. Rickert, E. Bamberg, H. J. Steinhoff, and C. Bamann, Angew. Chem. Int. Ed. Engl. **52**(37), 9705 (2013).
[89]M. Nack, I. Radu, M. Gossing, C. Bamann, E. Bamberg, G. F. von Mollard, and J. Heberle, Photochem. Photobiol. Sci. **9**(2), 194 (2010).
[90]V. A. Lórenz-Fonfría, T. Resler, N. Krause, M. Nack, M. Gossing, G. Fischer von Mollard, C. Bamann, E. Bamberg, R. Schlesinger, and J. Heberle, Proc. Natl. Acad. Sci. U.S.A. **110**(14), E1273 (2013).
[91]M. Nack, Ph.D. thesis, Freie Universitaet Berlin, 2012.

SUPPLEMENTAL MATERIAL

TO

Changes in the hydrogen-bonding strength of internal water molecules and cysteine residues in the conductive state of channelrhodopsin-1

Víctor A. Lórenz-Fonfría,*[a)] Vera Muders,*[b)] Ramona Schlesinger,[b)] Joachim Heberle[a]
[a)]Experimental Molecular Biophysics and [b)]Genetic Biophysics, Freie Universität Berlin, 14195 Berlin, Germany
* These authors contributed equally

I. Supplementary Figures

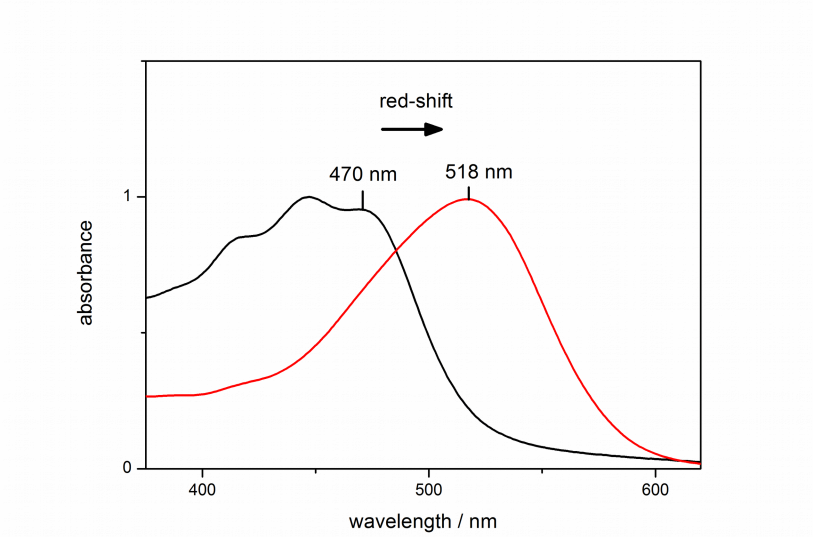

Fig. S1. Absorption spectra of *Cr*ChR2 (black) and *Ca*ChR1 (red) in the visible. The characteristic retinal peaks are displayed in the region between 380 - 620 nm. Note the red-shifted absorption maximum of *Ca*ChR1 as compared to *Cr*ChR2.

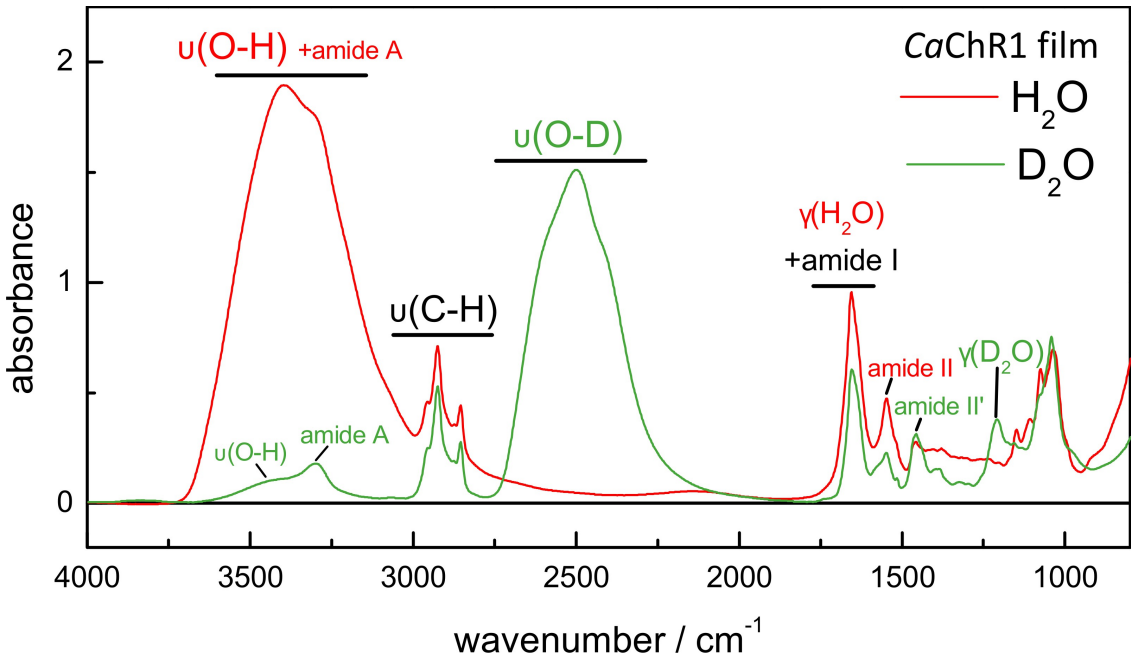

Fig. S2. Infrared absorption spectra of *Ca*ChR1 samples rehydrated with H_2O (red) and D_2O (green). Band assignments are given for bending and stretching vibrations of water and amide vibrations of the peptide bond.

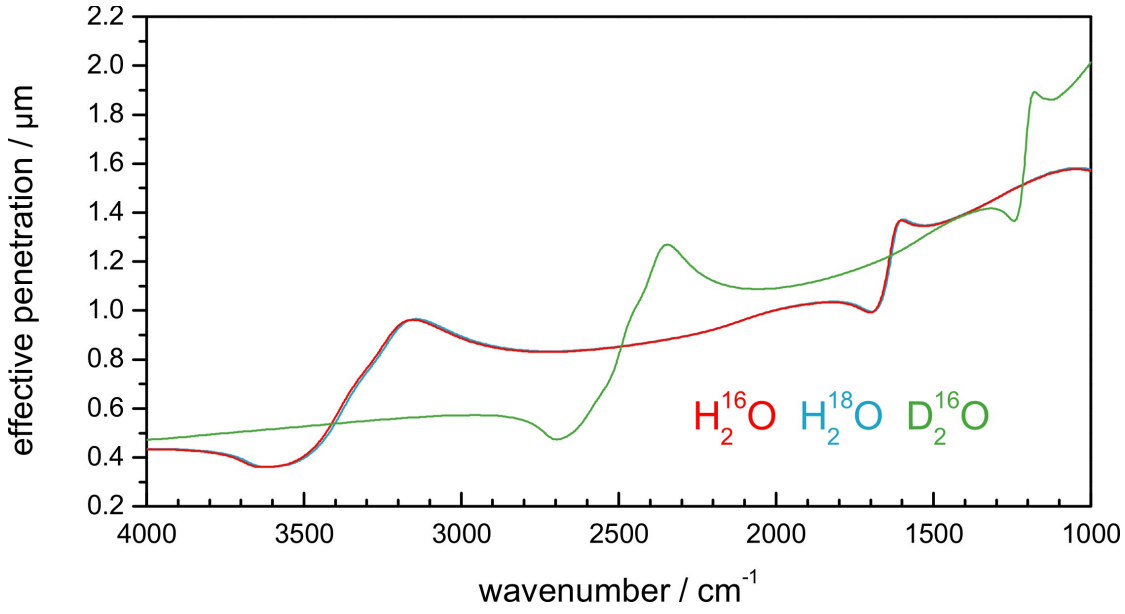

Fig. S3. Dependence of the effective depth of penetration, dp_e, on the wavenumber for water in a single-reflection attenuated total reflection setup. The penetration depth of the evanescent wave evoked by an unpolarized IR beam is given by: $dp_e = 0.5 \times dp_{e,0} + 0.5 \times dp_{e,90}$, where $dp_{e,0}$ and $dp_{e,90}$ are the effective penetration depths for parallel and perpendicular

polarized light. For the thick-film weak-absorber approximation of Harrick, the following equations are used:[1] $dp_{e,90}=\frac{n_2\times\langle E(0)^2\rangle_y\times dp}{2n_1\times\cos\theta}=\frac{n_{21}\cos\theta}{\pi n_1\nu\left(1-n_{21}^2\right)\sqrt{\sin^2\theta-n_{21}^2}}$ and $dp_{e,0}=\frac{n_2\times\left(\langle E(0)^2\rangle_x+\langle E(0)^2\rangle_z\right)\times dp}{2n_1\times\cos\theta}=\frac{n_{21}\cos\theta\left(2\sin^2\theta-n_{21}^2\right)}{\pi n_1\nu\left(1-n_{21}^2\right)\left[\left(1+n_{21}^2\right)\sin^2\theta-n_{21}^2\right]\sqrt{\sin^2\theta-n_{21}^2}}$, where n_2 and n_1 are the refractive indices of the sample (water) and the material of the internal reflection element (diamond), respectively, and $n_{21} = n_2/n_1$; θ is the angle of incidence of the IR beam with respect to the surface of the reflection element (45°); $\langle E(0)^2\rangle_{x,y,\vee z}$ is the initial intensity of the evanescent electric field relative to the incident intensity of the IR beam in the directions *x*, *y*, and *z* (see Fig. 1 in [1]); *dp* is the penetration depth of the evanescent wave, $dp=\left(2\pi n_1\nu\sqrt{\sin^2\theta-\left(n_2/n_1\right)^2}\right)$; and ν is the wavenumber of the incident light in vacuum. For n_2, the refractive index of water as a function of the wavenumber was used.[2]

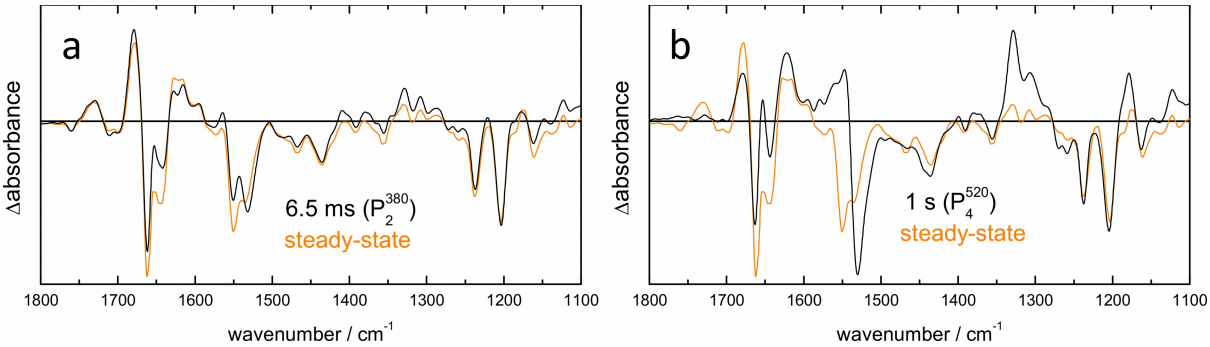

Fig. S4. Comparison of the steady-state FT-IR difference spectrum (continuous illumination with LED) with time-resolved rapid-scan FT-IR difference spectra (nanosecond laser pulse excitation) at (a) 6.5 ms (P_2^{380} intermediate) and at (b) 1 s (P_4^{520}) after excitation. We can conclude that the P_2^{380} intermediate is predominantly accumulated under continuous illumination. All spectra are at 8 cm^{-1} instrumental resolution, scaled at the negative bands at 1,237 and 1,202 cm^{-1} of the retinal fingerprint.

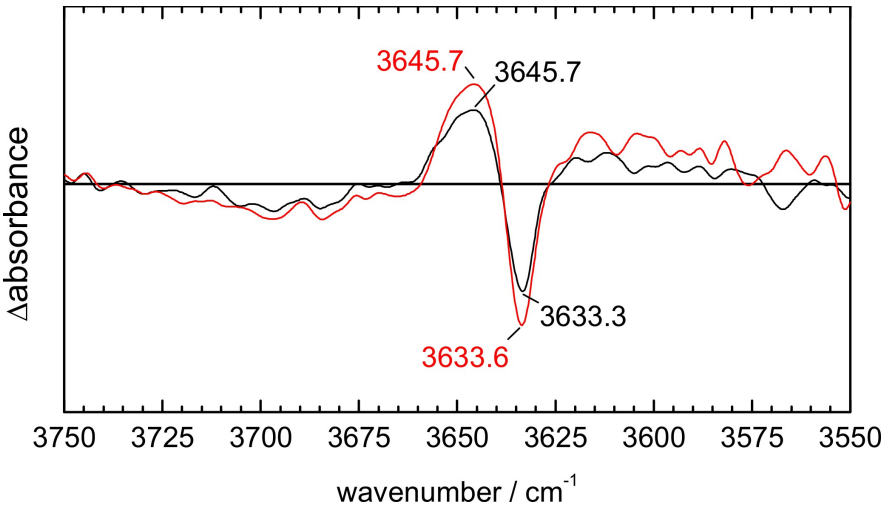

Fig. S5. Steady-state FT-IR spectrum of *Ca*ChR1 from two independent measurements (performed on films from different protein stocks). Both spectra were subjected to an identical baseline correction procedure to remove contributions from water heating. Bands assigned to dangling O-H stretches of water are shown and their wavenumber maximum labeled. Note the high reproducibility of the band maximum wavenumber.

References

[1] E. Goormaghtigh, V. Raussens, and J. M. Ruysschaert, Biochim. Biophys. Acta **1422** (2), 105 (1999).

[2] J. E. Bertie and M. K. Ahmed, J. Phys. Chem. **93**, 2210 (1989); J. E. Bertie and Z. D. Lan, Appl. Spectrosc. **50** (8), 1047 (1996).